Original Article

Clinicopathological and computed tomography features associated with recurrence-free survival of patients with small-sized peripheral invasive lung adenocarcinoma after sublobectomy

Jiwen Huo^, Tianyou Luo^, Fajin Lv^, Qi Li^

Department of Radiology, the First Affiliated Hospital of Chongqing Medical University, Chongqing, China

Contributions: (I) Conception and design: Q Li; (II) Administrative support: T Luo, F Lv; (III) Provision of study materials or patients: Q Li, T Luo, F Lv; (IV) Collection and assembly of data: J Huo; (V) Data analysis and interpretation: J Huo, Q Li; (VI) Manuscript writing: All authors; (VII) Final approval of manuscript: All authors.

Correspondence to: Qi Li, MD. Department of Radiology, the First Affiliated Hospital of Chongqing Medical University, No. 1 Youyi Road, Yuzhong District, Chongqing 400016, China. Email: 202770@hospital.cqmu.edu.cn.

Background: Sublobar resection is gradually becoming a standard treatment for small-sized (≤2 cm) peripheral non-small cell lung cancer (NSCLC), with lung adenocarcinoma (LADC) being the most frequent histologic subtype. However, the prognostic predictors for preoperatively determining whether sublobectomy is feasible for patients with early LADC have not yet been well identified. Therefore, this study aimed to investigate the clinicopathological and computed tomography (CT) features associated with the recurrence-free survival (RFS) of patients with small-sized invasive LADC (SILADC) after sublobar resection.

Methods: This retrospective cohort study analyzed 107 patients with SILADC who underwent preoperative chest CT scan and sublobar resection from December 2012 to March 2019. The Kaplan-Meier survival was used to analyze the relationship between clinicopathological characteristics, preoperative chest CT findings, and RFS. The Cox proportional hazards regression was used to identify independent prognostic factors of poor RFS.

Results: For clinicopathological characteristics, RFS was shorter in patients aged ≥70 years, smokers, and those with micropapillary/solid-predominant adenocarcinomas (all P values <0.05). For preoperative CT features, RFS was shorter in patients with tumor size ≥1.4 cm, solid component size ≥1.1 cm, proportion of solid component ≥72%, solid density, spiculation, vascular convergence sign, peripheral fibrosis, and type II pleural tag (all P values <0.05). Multivariate analysis showed proportion of solid component ≥72% [hazard ratio (HR): 5.920; P=0.006; 95% confidence interval (CI): 1.686–20.794], spiculation (HR: 5.026; P=0.001; 95% CI: 2.008–12.581), and type II pleural tag (HR: 4.638; P=0.002; 95% CI: 1.773–12.136) were independent risk factors for poor prognosis in patients with SILADC after sub-lobectomy.

Conclusions: Clinicopathological and CT characteristics are helpful for predicting the RFS of patients with SILADC after sublobar resection and can be used as an auxiliary tool for thoracic surgeons to choose the best surgical mode.

Keywords: Lung cancer; adenocarcinoma; computed tomography (CT); sublobectomy; prognosis

Submitted Apr 22, 2023. Accepted for publication Sep 22, 2023. Published online Oct 16, 2023.
doi: 10.21037/qims-23-559
View this article at: https://dx.doi.org/10.21037/qims-23-559

^ ORCID: Jiwen Huo, 0000-0002-2996-4175; Tianyou Luo, 0000-0002-5251-8667; Fajin Lv, 0000-0002-6484-9738; Qi Li, 0000-0002-9452-925X.

Introduction

Lung cancer continues to be the leading cause of cancer-related mortality worldwide, and about 85% of the cases are non-small cell lung cancer (NSCLC), with the most common histologic subtype being lung adenocarcinoma (LADC) in the overall reported cases (1). With the popularization of low-dose computed tomography (CT) screening, the detection rate of early lung cancer is increasing remarkably (2,3). Currently, surgical radical resection remains the mainstay treatment for early LADC. As the world's population continues to age and surgical technology continues to advance, the need for minimally invasive treatment is increasing, with sublobar resection (wedge resection or anatomical segmentectomy) being more widely used in the treatment of early lung cancer with small tumor size (4,5). Compared with lobectomy, sublobectomy can better preserve the patient's lung function; reduce the damage to normal lymph nodes, hilar, and mediastinum; and potentially allow for reoperation in the future. however, it may also lead to an undesirable survival outcome in some patients due to incomplete tumor resection (6-8).

Several studies have demonstrated that sublobectomy achieves similar survival outcomes compared to lobectomy in suitably selected patients (7-9). A recent multicenter randomized trial (JCOG0802) spearheaded by Saji *et al.* (8) reported that for patients with clinical stage IA NSCLC (tumor size ≤2 cm), anatomical segmentectomy yielded superior overall survival rates and was on par with lobectomy in terms of recurrence-free survival (RFS). Another randomized trial conducted by Altorki *et al.* (9) demonstrated that for patients with peripheral clinical stage T1aN0 NSCLC, sublobar resection was equivalent to lobectomy in terms of disease-free survival, and overall survival rates were comparable between the two procedures. As outlined in the 2022 National Comprehensive Cancer Network's Clinical Practice Guidelines in NSCLC (available at https://www.nccn.org/), sublobectomy may be a suitable surgical option for patients with compromised cardiopulmonary function or for those with peripheral tumors with a diameter ≤2 cm. The latter group also needs to meet 1 of the following conditions: ground-glass opacity (GGO) component ≥50%, tumor doubling time >400 days upon long-term follow-up, or presentation of *in situ* or minimally invasive LADC (ILADC) (10). However, the efficacy and advantages of sublobectomy in early-stage ILADC have not yet been comprehensively established, leaving the patient outcomes somewhat uncertain. For patients with early ILADC, insight into the clinicopathological and imaging features in relation to their RFS after sublobar resection may be particularly helpful in further stratifying these patients and in guiding their clinical management (11,12).

Therefore, this study aimed to investigate the value of clinicopathological and CT characteristics to preoperatively predict the RFS of patients with small-sized ILADC (SILADC) after sublobar resection, potentially providing an auxiliary tool for thoracic surgeons for identifying patients that might benefit from this treatment strategy. We present this article in accordance with the STROBE reporting checklist (available at https://qims.amegroups.com/article/view/10.21037/qims-23-559/rc).

Methods

Patients

The study was conducted in accordance with the Declaration of Helsinki (as revised in 2013) and was approved by the ethics committee of The First Affiliated Hospital of Chongqing Medical University. The need for an informed consent was waived due to its retrospective nature. A total of 2,401 patients confirmed with LADC from December 2012 to March 2019 were initially included. The inclusion criteria were as follows: (I) pathological confirmation of LADC; (II) history of sublobar resection (wedge resection or segmentectomy); (III) CT scanning prior to surgery; (IV) clinical stage IA with tumor size ≤2 cm on CT images; and (V) a follow-up period of at least 3 years after surgery. Of the patients initially included, 2,294 with LADC were excluded according to the following exclusion criteria: (I) patients were pathologically confirmed with carcinoma *in situ* or minimally ILADC; (II) patients had multiple primary lung cancers; (III) CT images lacked of adequate quality for diagnosis; and (IV) clinical data were unavailable. Consequently, this study included 107 patients with SILADC. The flow diagram for this study is provided in *Figure 1*. Furthermore, clinicopathologic data (including age, gender, smoking history, and histological subtype) were collected from the medical records.

CT scanning protocol

All patients underwent preoperative chest CT scan with

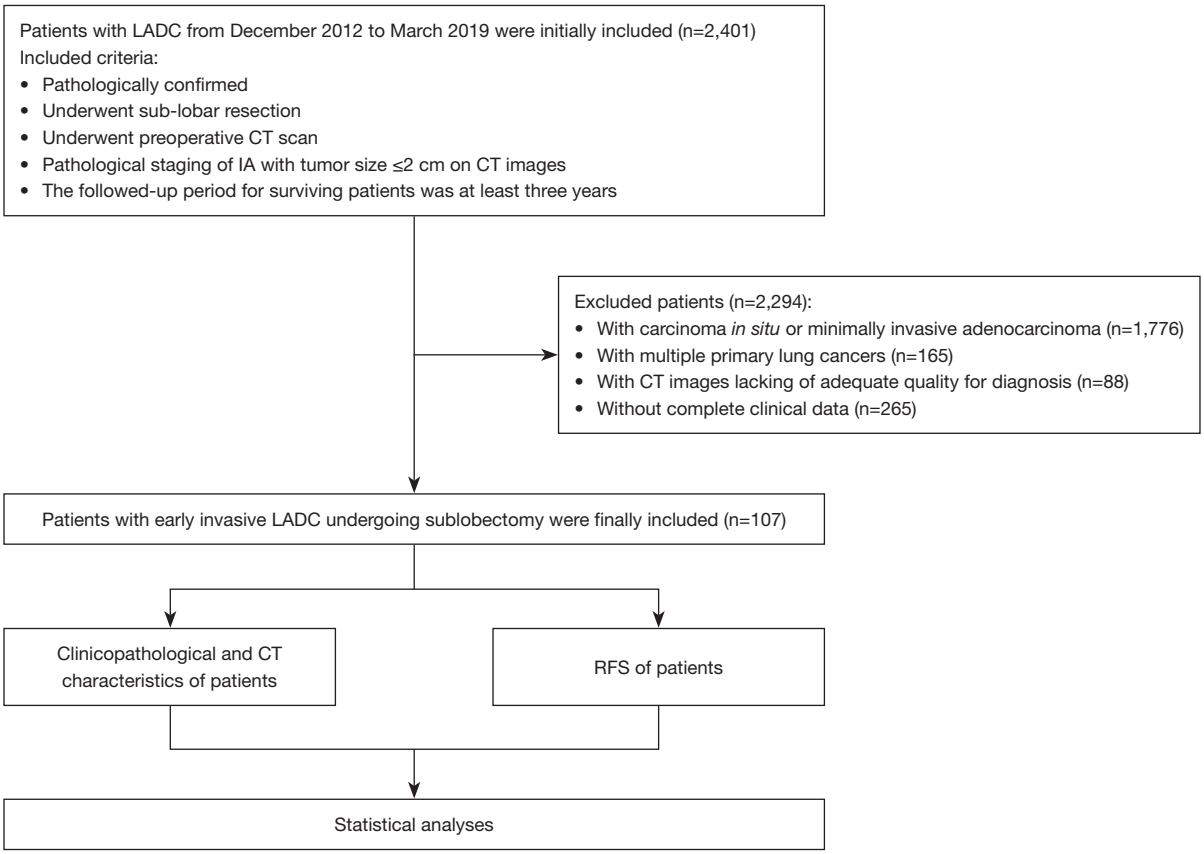

Figure 1 The flow diagram for the patient selection and the data analysis followed in this study. LADC, lung adenocarcinoma; CT, computed tomography; RFS, recurrence-free survival.

a GE Discovery 750 HD (GE HealthCare, Chicago, IL, USA) or SOMATOM Definition Flash (Siemens Healthineers, Erlangen, Germany) scanner. Unenhanced CT scanning was conducted first. The scanning range covered the entire chest from the first rib to the diaphragm. The CT scanning parameters were as follows: tube voltage, 120–140 kV; tube current, 100–250 mA; and slice thickness/interval, 5 mm/5 mm. The patients were then injected with a nonionic iodinated contrast medium (iohexol; 300 mg iodine/mL) via a double high-pressure syringe (at a flow rate of 3.0 mL/s) through the anterior cubital vein at a dose of 1.5 mL/kg (total volume: 80–110 mL), followed by 50 mL of a saline solution. The acquisition times in the arterial and the delayed phase were triggered at 30 and 120 s, respectively, after the start of the contrast medium injection. Subsequently, all images were reconstructed with a slice thickness of 0.625–1.25 mm and a slice interval of 0.625–1.25 mm and were transmitted to the Picture Archiving and Communication System (PACS) workstation (Vue PACS, Carestream, Rochester, NY, USA).

CT image interpretation

Two radiologists with >10 years of experience in thoracic radiology were blinded to the related clinical data and evaluated CT images independently on a PACS workstation. In case of any discrepancy, a consensus was reached by discussion, and the results agreed upon were used for further analysis. The CT morphological features of the tumors were carefully analyzed as follows: (I) tumor and solid component sizes (tumor size: the maximum diameter of the tumor in the multiplanar recombination on the lung window setting; solid component size: the maximum diameter of the solid component within the tumor in the multiplanar recombination on the lung window setting); (II) location (right upper, middle, and lower lobes; left

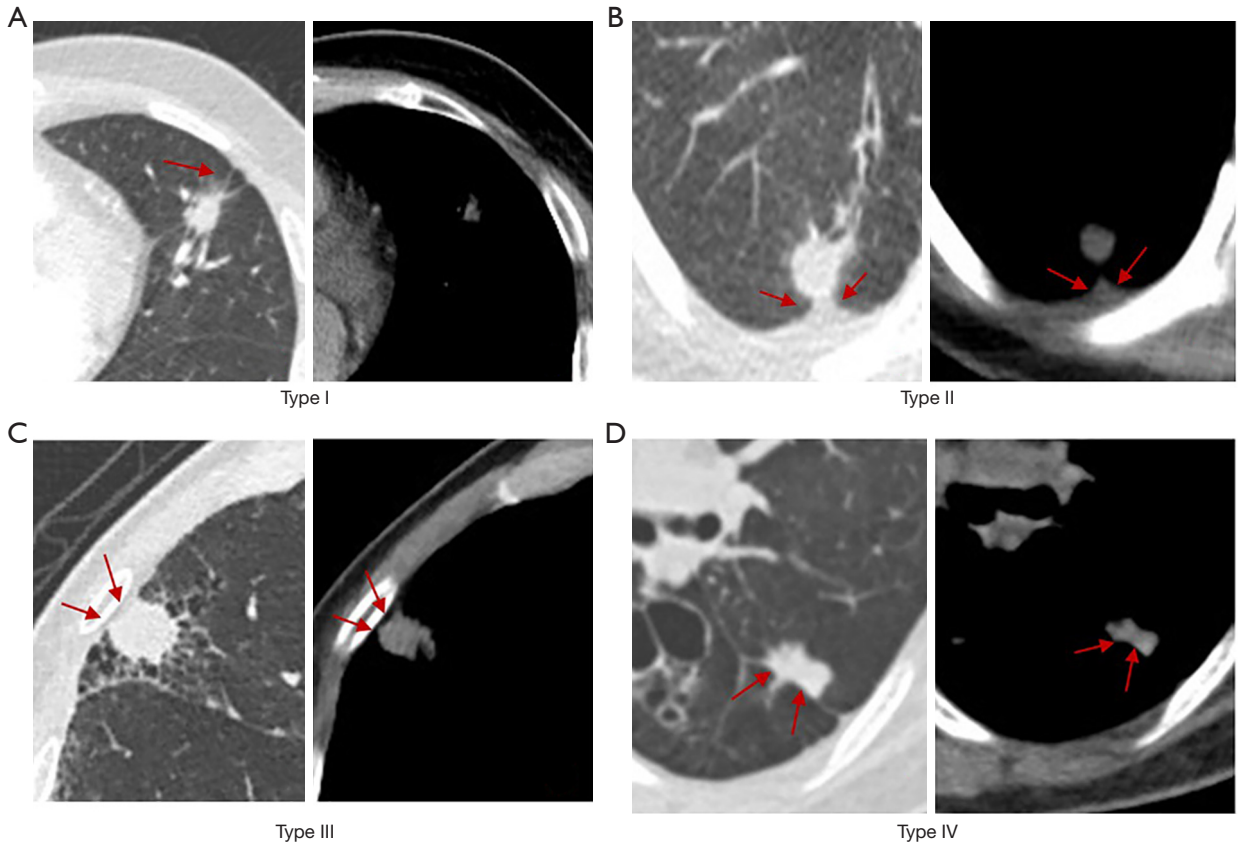

Figure 2 Representative CT images of pleural tag in SILADC. SILADC with pleural tag of type I (A), type II (B), type III (C), and type IV (D) (red arrows) on lung and mediastinal window images. CT, computed tomography; SILADC, small-sized invasive lung adenocarcinoma.

upper and lower lobes); (III) density (subsolid: tumor with a component of GGO defined as a hazy increased opacity with preservation of bronchial and vascular margins; solid: tumor without GGO); (IV) proportion of solid component (%; the ratio of solid component size/tumor size); (V) shape (regular: round or oval; irregular: with an uneven contour that could not be identified as round or oval); (VI) margin (spiculation and lobulation); (VII) internal characteristics (air bronchogram: air-filled bronchus within the tumor; air space: air attenuation density within the tumor, including cavity and pseudocavity); and (VIII) external characteristics [vascular convergence sign: vessels around the tumor gathered together and broken at the tumor or penetrating the tumor; peripheral fibrosis: peripheral fibrosis caused by the tumor or preexisting fibrosis (13); pleural tag (*Figure 2*): type I, one or more linear-like structures connected between the tumor and pleural and present in the lung but not in the mediastinal window images; type II, pleural retraction with thickening at the pleural end, but not at the fissure, present in both the lung and mediastinal window images; type III, tumor attaching to the pleura but not the fissure, with the tumor margin obscured by the pleura; type IV, tumor attaching to the fissure.

Follow-up

The postoperative follow-up data of patients were obtained from outpatient and telephone follow-up. According to the follow-up protocol of our institution, patients underwent chest CT scans at 3 and 6 months postoperatively and every 6 months thereafter. The last follow-up date was March 24, 2022. The RFS was the end point of this study, and it was defined from the date of sublobectomy to either the date of recurrence (event) or the date that the patient was last known to be free of recurrence (censored). Recurrence referred to local, regional, locoregional,

and distant recurrence. Local recurrence was defined as recurrence within the primary tumor lobe at the staple line (local progression), recurrence within the primary tumor lobe away from the staple line (involved lobe failure), or recurrence within the ipsilateral hilar lymph nodes; regional recurrence was defined as recurrence within another lobe on the same side as the resection or within the ipsilateral mediastinal or subcarinal lymph nodes; locoregional recurrence was defined as the combination of local and regional recurrence; and distant recurrence was defined as recurrence within the contralateral lung, mediastinal, or hilar lymph nodes or distant metastatic disease. The minimum follow-up period for the identification of the RFS was 2.7 months after sublobar resection, while the maximum follow-up period was 72.1 months, and the median follow-up period of all patients was 40.4 months.

Statistical analysis

All statistical analyses were performed with the SPSS 25.0 software (version 25.0, IBM Corp., Armonk, NY, USA). The age and the follow-up time were normally distributed and evaluated by using independent samples *t*-test. For tumor size, solid component size, and proportion of the solid component, the Youden indices were calculated to establish the optimal threshold values. The relationships between the clinicopathological and CT features and the RFS were assessed using the Kaplan-Meier survival analysis and the log-rank test, and missing data were censored. The independent risk prognostic factors were determined with the Cox proportional hazards regression analysis using clinical and CT features demonstrated with statistical significance in univariate analysis. A two-tailed P value of <0.05 was considered to indicate a statistical significance. In addition, the intraclass correlation coefficient (ICC) was used to evaluate the diagnostic consistency of the CT features of tumor, and an ICC value >0.75 was considered as indicative of a good agreement between the two observers.

Results

Observer reproducibility

The agreement between the two observers was fairly good for all CT features. The ICC values for the tumor size, solid component size, proportion of solid component, density, shape, spiculation, lobulation, air bronchogram, air space, vascular convergence sign, peripheral fibrosis, pleural tag type I, pleural tag type II, pleural tag type III, and pleural tag type IV were 0.942, 0.926, 0.931, 0.935, 0.898, 0.853, 0.841, 0.951, 0.954, 0.836, 0.935, 0.979, 0.929, 0.934, and 0.938, respectively (all P values <0.001).

Patient characteristics

A total of 107 patients with SILADC that underwent sublobectomy were analyzed; wedge resection was performed in 59 patients (55.1%) and segmentectomy in 48 patients (44.9%). Moreover, 87 patients (81.3%) were clinical stage of T1a and 20 (18.7%) were T1b. The patients' mean age was 63.9±11.0 years, and the age range was from 24 to 83 years. Regarding the LADC histological subtypes, 68.2% (73/107) of the patients had an acinar-predominant subtype, 20.6% (22/107) had a lepidic-predominant subtype, 5.6% (6/107) had a papillary-predominant subtype, 4.7% (5/107) had a solid-predominant subtype, and 0.9% (1/107) had a micropapillary-predominant subtype. Additionally, 63 patients underwent intraoperative sampling of the hilar and mediastinal lymph nodes, and none had lymph node metastasis, whereas 44 patients did not undergo sampling due to poor lung function. The patients' clinicopathological characteristics are listed in *Table 1*. The mean follow-up period of all patients was 39.9±14.5 months. During the follow-up period, 23 patients experienced relapse, including eight with local recurrence, six with regional recurrence, four with locoregional recurrence, and five with distant recurrence; the 1-, 2-, and 3-year RFS rates of these patients were 95.3% (102/107), 86.9% (93/107), and 80.4% (86/107), respectively.

Relationship between clinicopathological characteristics and RFS

As delineated in *Table 1*, the RFS was shorter in patients aged ≥70 years, smokers, and those with micropapillary/solid-predominant adenocarcinomas (all P values <0.05). No significant differences were found in the RFS between male and female patients, between undergoing segmentectomy and wedge resection, or between clinical stage of T1a and T1b (all P values >0.05).

Relationship between preoperative CT characteristics and RFS

As seen in *Table 2*, the RFS was shorter in patients with tumor size ≥1.4 cm, solid component size ≥1.1 cm,

Table 1 Relationship between clinicopathological characteristics and RFS in patients with SILADC undergoing sublobectomy

Characteristics	Patients (n=107)	Mean RFS (months)	Median RFS (months)	P value
Age				0.009
≥70 years	36 (33.6)	50.6±4.1	NE	
<70 years	71 (66.4)	65.2±2.2	NE	
Sex				0.083
Male	53 (49.5)	56.4±3.3	NE	
Female	54 (50.5)	64.9±2.6	NE	
Smoking				0.011
Smokers	41 (38.3)	52.2±3.9	NE	
Non-smokers	66 (61.7)	65.6±2.2	NE	
Histological subtype				<0.001
Micropapillary/solid-predominant subtypes	6 (5.6)	24.9±9.1	12.5±9.1	
Lepidic/acinar/papillary-predominant subtypes	101 (94.4)	63.5±2.0	NE	
Surgical method				0.070
Segmentectomy	48 (44.9)	62.1±2.2	NE	
Wedge resection	59 (55.1)	55.8±2.2	68.8±12.5	
Tumor clinical stage				0.213
T1a	87 (81.3)	66.2±2.8	NE	
T1b	20 (18.7)	59.9±2.5	NE	

Number of patients are presented as n (%); mean and median RFSs of patients are presented as mean ± standard deviation and median ± interquartile range, respectively. RFS, recurrence-free survival; SILADC, small-sized invasive lung adenocarcinoma; NE, not evaluated.

proportion of solid component ≥72%, solid density, spiculation, vascular convergence sign, peripheral fibrosis, and type II pleural tag (all P values <0.05) (*Figure 3*).

The cutoff values of tumor size, solid component size, and proportion of solid component were 1.4 cm, 1.1 cm, and 72%, with areas under the curve (AUCs) of 0.626, 0.734, and 0.772, respectively. No significant differences were observed in the RFS between patients with tumors of different locations and shapes or and between those with and without lobulated tumors, air bronchogram, air space, or type I/III/IV pleural tags (all P values >0.05). The Kaplan-Meier survival curves of the analyzed patients are presented in *Figure 4*.

Prognostic factor analysis

The Cox analysis revealed that the proportion of solid component [hazard ratio (HR): 5.920; P=0.006; 95% confidence interval (CI): 1.686–20.794], spiculation (HR: 5.026; P=0.001; 95% CI: 2.008–12.581), and type II pleural tag (HR: 4.638; P=0.002; 95% CI: 1.773–12.136) were independent risk factors for the poor prognosis of patients with SILADC after sublobar resection (*Table 3*).

Discussion

For patients diagnosed with peripheral early-stage lung cancer, especially for those at an advanced age, with poor cardiopulmonary function, or experiencing significant complications, appropriate criteria for selecting those who will undergo a sublobar resection are crucial. In this study, we characterized the clinicopathological and CT features conducive to selecting sublobectomy for patients with SILADC. Several major findings were identified.

First, we examined the correlation between clinicopathological characteristics and RFS for patients with SILADC who underwent sublobar resection. We found that patients aged <70 years had a better prognosis

Table 2 Relationship between CT features and RFS in patients with SILADC undergoing sub-lobectomy

Characteristics	Patients (n=107)	Mean RFS (months)	Median RFS (months)	P value
Location				0.952
Right upper lobe	43 (40.2)	59.3±3.3	NE	
Right middle lobe	6 (5.6)	59.5±8.5	NE	
Right lower lobe	15 (14.0)	64.5±3.0	NE	
Left upper lobe	31 (29.0)	58.4±4.2	NE	
Left lower lobe	12 (11.2)	48.7±5.1	NE	
Tumor size				0.010
≥1.4 cm	67 (62.6)	55.2±3.1	68.8±1.1	
<1.4 cm	40 (37.4)	66.8±2.0	NE	
Solid component size				<0.001
≥1.1 cm	43 (40.2)	48.8±4.1	67.6±20.2	
<1.1 cm	64 (59.8)	68.0±1.8	NE	
Proportion of solid component				<0.001
≥72%	45 (42.1)	47.3±4.0	67.6±16.9	
<72%	62 (57.9)	69.7±1.4	NE	
Density				<0.001
Solid	29 (27.1)	45.1±5.0	NE	
Subsolid	78 (72.9)	66.7±1.8	NE	
Shape				0.080
Regular	80 (74.8)	58.0±2.5	NE	
Irregular	27 (25.2)	67.4±3.2	NE	
Spiculation	19 (17.8)	36.1±6.3	24.4±6.0	<0.001
Lobulation	95 (88.8)	59.3±2.3	NE	0.332
Air bronchogram	19 (17.8)	63.3±4.6	NE	0.650
Air space	31 (29.0)	52.7±2.2	NE	0.109
Vascular convergence sign	24 (22.4)	41.4±4.9	NE	<0.001
Peripheral fibrosis	27 (25.2)	44.3±5.1	NE	<0.001
Pleural tag				
Type I	36 (33.6)	61.4±3.7	NE	0.984
Type II	11 (10.3)	37.6±8.4	25.0±0.0	<0.001
Type III	12 (11.2)	44.0±5.3	NE	0.213
Type IV	13 (12.1)	50.9±1.8	NE	0.249

Number of patients are presented as n (%); mean and median RFSs of patients are presented as mean ± standard deviation and median ± interquartile range, respectively. CT, computed tomography; RFS, recurrence-free survival; SILADC, small-sized invasive lung adenocarcinoma; NE, not evaluated.

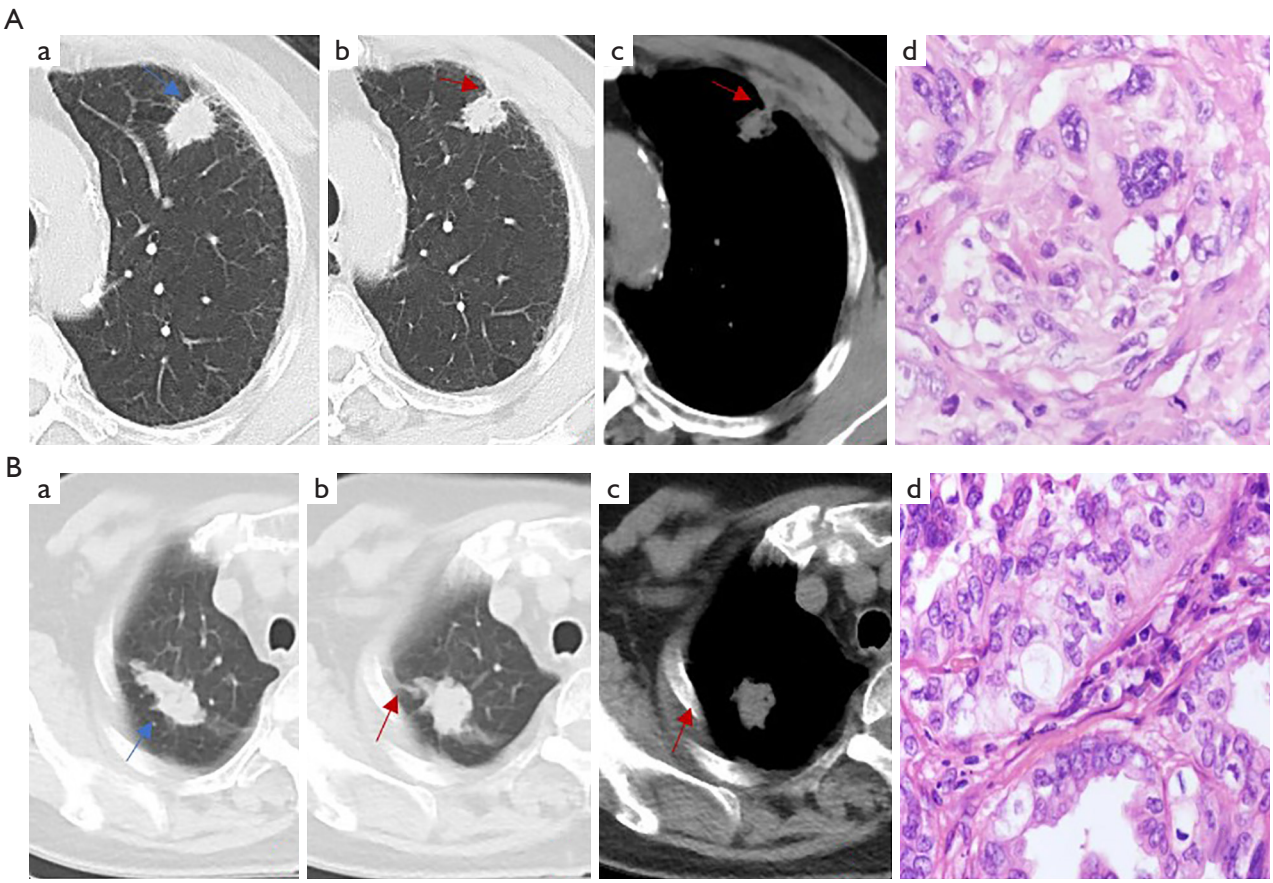

Figure 3 CT features and histological subtypes of SILADC cases with different RFS after sub-lobectomy. (A) A 72-year-old man with SILADC, whose sublobectomy took place on January 20, 2017, and the date of relapse was December 6, 2018, with a RFS of 12.5 months. (a-c) Axial CT images of the lung and the mediastinal window setting reveal a solid nodule with spiculation (blue arrow) and type II of pleural tag (red arrows) in the left upper lobe. (d) Photomicrograph (hematoxylin and eosin staining, ×400) of histopathology confirms the SILADC diagnosis with a solid-predominant growth pattern. (B) A 72-year-old man with SILADC, whose sub-lobectomy took place on July 13, 2017, and the last assessed recurrence-free date was March 24, 2022, with a RFS of 56.4 months. (a-c) Axial CT images of the lung and the mediastinal window setting reveal a solid nodule with an irregular shape (blue arrow) and type I of pleural tag (red arrows) in the right upper lobe. (d) Photomicrograph (hematoxylin and eosin staining, ×400) of histopathology confirms the SILADC diagnosis with an acinar-predominant growth pattern. CT, computed tomography; SILADC, small-sized invasive lung adenocarcinoma; RFS, recurrence-free survival.

than did those aged ≥70 years, which is similar to the results reported by Saji *et al.* (8). Our results also indicated that smokers had a shorter RFS than did non-smokers. A few recent studies reported the relationships between smoking history and prognosis after sublobar resection. Mimae *et al.* (14) assessed the prognosis of 669 patients with clinical stage IA NSCLC undergoing wedge resection and revealed that smoking history was not associated with patient outcome. However, Huang *et al.* showed that early lung cancer patients with smoking history might be at high risk of recurrence, which is consistent with our findings (15). The conflicting results from those studies may be attributed to the study sample size and a difference in ethnicity. Furthermore, we found that patients with micropapillary/solid-predominant adenocarcinomas usually had a worse prognosis than did those with lepidic, acinar, or papillary-predominant adenocarcinomas. Generally, the micropapillary-predominant growth pattern is mostly composed of papillary tufts and is lacking fibrovascular cores; the micro-papillae may be folding on alveolar surfaces, floating within the alveoli, and sometimes infiltrating the stroma as small clusters; on the other hand,

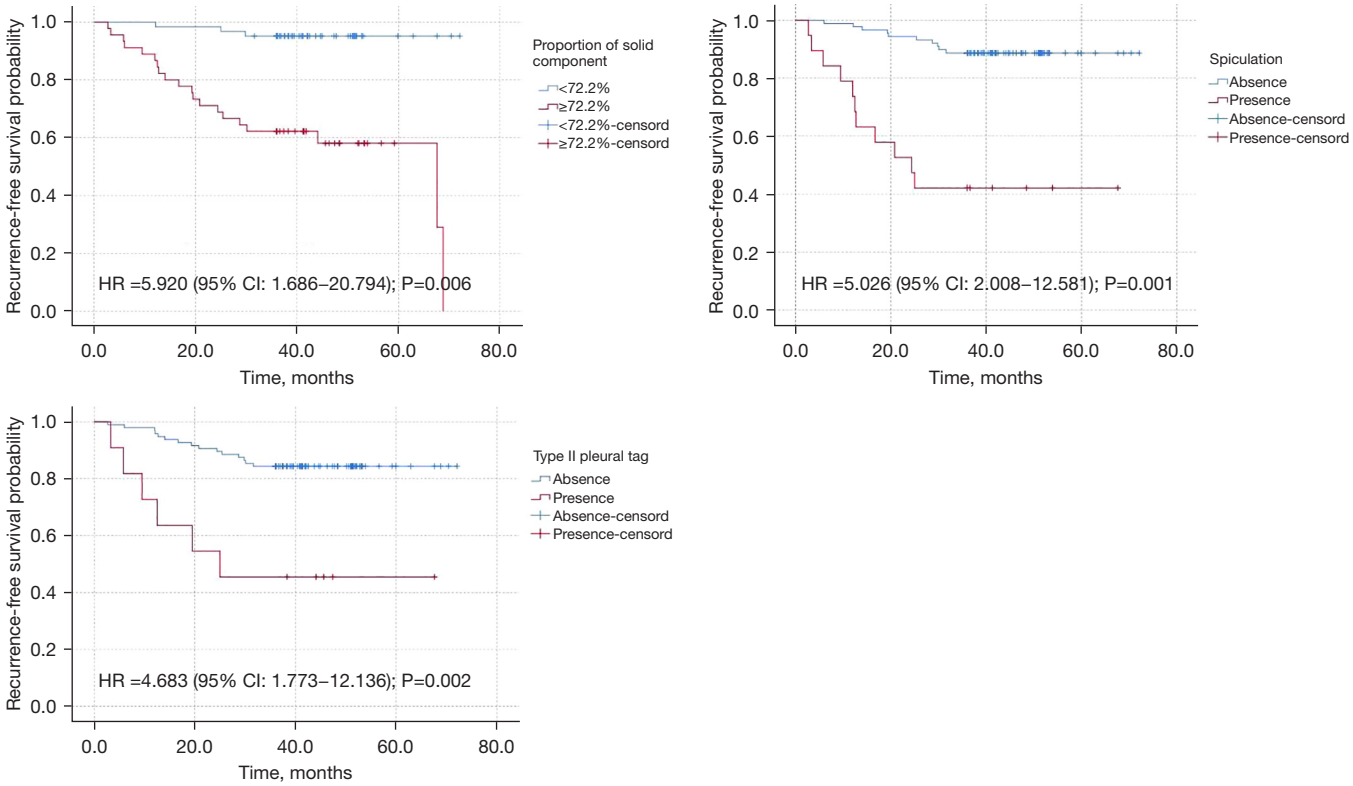

Figure 4 The Kaplan-Meier survival curves for SILADC patients with different clinicopathological and CT characteristics. HR, hazard ratio; CI, confidence interval; SILADC, small-sized invasive lung adenocarcinoma; CT, computed tomography.

Table 3 Univariate and multivariate survival analysis of prognostic factors in patients with SILADC undergoing sub-lobectomy

CT features	Univariate analysis			Multivariate analysis		
	HR	95% CI	P value	HR	95% CI	P value
Age ≥70 years	3.361	1.432–7.887	0.005			
Smokers	2.779	1.202–6.426	0.17			
Tumor size ≥1.4 cm	4.298	1.275–14.491	0.019			
Solid component size ≥1.1 cm	6.219	2.303–16.796	<0.001			
Proportion of solid component ≥72%	11.378	3.377–38.330	<0.001	5.920	1.686–20.794	0.006*
Solid density	6.006	2.535–14.228	<0.001			
Spiculation	7.908	3.335–18.749	<0.001	5.026	2.008–12.581	0.001*
Vascular convergence sign	4.83	2.048–11.435	<0.001			
Peripheral fibrosis	5.059	2.127–12.029	<0.001			
Type II pleural tag	5.072	1.959–13.128	0.001	4.638	1.773–12.136	0.002*

*, variables included in the equation. SILADC, small-sized invasive lung adenocarcinoma; HR, hazard ratio; CI, confidence interval.

the solid-predominant growth pattern is mostly composed of solid nests, which are generally not conducive to histological differentiation and tend to grow faster (16,17). Therefore, micropapillary- and solid-predominant patterns of adenocarcinoma are likely associated with tumor relapse. Previous studies have revealed the prognostic relevance of histological subtypes in early LADC (18-20). According to these studies, patients with lepidic-predominant subtypes are strongly associated with a good prognosis, those with acinar/papillary-predominant subtypes are usually related with an intermediate prognosis (18,19), and those with micropapillary/solid-predominant subtypes tend to have a poor outcome (20), which corroborates our findings. However, histological subtypes of tumors can be available during or—in most cases—after the operation. As it is generally difficult to determine the growth patterns of ILADC via intraoperative frozen section, the histopathological subtypes of ILADC were not included in the Cox proportional hazards regression analysis in identifying those factors most associated with poor RFS in patients with SILADC before surgery.

Subsequently, we investigated the preoperative CT features of patients with SILADC in relation to postoperative recurrence. First, our results demonstrated that patients with SILADC with a tumor size ≥1.4 cm tended to have a worse prognosis. Moon *et al.* (21) indicated that larger tumor size is a significant risk factor for recurrence in patients with small-tumor NSCLC manifesting as solid-predominant nodule after sublobar resection, which is in line with our findings. Second, we found SILADC with solid component size ≥1.1 cm, proportion of solid component ≥72%, and solid density were highly indicative of a poor outcome. Previous studies have revealed that GGO components within tumors are closely related to the lepidic-predominant growth pattern, which is highly suggestive of a favorable prognosis (16,22,23), whereas solid components within tumors are more likely to be related to other patterns, which have a relatively poor prognosis (17,24-26); this may be a good explanation for our findings. Moreover, this study demonstrated that tumors with spiculation, vascular convergence sign, peripheral fibrosis, and type II pleural tag were associated with a shorter RFS. Spiculation manifests as lines radiating from the tumor margins to the surrounding lung parenchyma and correlates with the fibrous tissue produced by tumor cells or tumor invasion along the adjacent bronchi, blood vessels, lymphatic vessels, or interlobular septum; thus, this sign may be associated with postoperative recurrence (27-30). Moreover, vascular convergence is a reflection of angiogenesis, which plays a critical role in the growth, progression, invasion, and metastasis of lung cancer (17). Ma *et al.* (31) reported that patients whose tumor presented with a vascular convergence sign had a poorer 5-year survival rate than did those whose tumor did not present with this sign, which is in agreement with our findings. Peripheral fibrosis may be related to tumor desmoplastic reaction and locoregional infiltration (13), and a tumor with this sign may exhibit aggressive behavior (32), which is in line with our study. Type II pleural tag is also known as pleural retraction and is closely related to the tumor contraction caused by the narrowing or collapse of alveolar spaces or from fibrotic areas in tumors (33). It is generally known that the visceral pleura is rich in lymphatic vessels forming an intercommunicating network over the lung surface and that this network penetrates the lung parenchyma and connects to the bronchial lymph vessels that drain into various hilar lymph nodes (34). Previous studies have indicated that pathologic visceral pleural invasion (PVPI) is highly indicative of poor prognosis in NSCLC, which significantly correlates with type II and III pleural tag based on CT (35,36); this is partly supported by our findings. We also found that unlike type II pleural tag, type III was not associated with the RFS of patients with SILADC. The different outcomes reported in the literature may be attributed to the heterogeneity in patients' inclusion criteria. The current study mainly focused on early ILADCs with small size, which usually have a lower probability of contacting the pleura as compared to larger tumors. Additionally, we found that the type IV pleural tag, which is characterized by a tumor attaching to the fissure, was not a reliable sign for predicting a short RFS. The reason for this may be that these lymphatics adjacent to the fissure may be less permeable to the tumor cells compared to those adjacent to the pleura, and thus tumors with such a sign are less likely to recur (36).

Finally, we built a multivariate Cox proportional hazards model in order to further identify the clinical and CT features that might prove helpful in selecting patients with SILADC for sublobar resection. Our results revealed that proportion of solid component ≥72%, spiculation, and type II pleural tag were independently associated with a poor prognosis, with HRs of 5.920, 5.026, and 4.638, respectively. Therefore, patients with SILADC and the aforementioned poor prognostic indicators should be considered with extreme caution in the decision to perform sublobar resection.

Our study has several limitations. First, the retrospective nature of this study deprived it of some detailed clinical data that could have also influenced the patients' survival. Second, the patient cohort was not large. Third, given that it is difficult to obtain pathological information preoperatively, this study did not include some pathological information associated with prognosis, such as lymphovascular invasion and visceral pleural invasion. Future studies with larger sample sizes are required to strengthen the reliability of the present findings.

Conclusions

In conclusion, clinicopathological and CT features are helpful in prognosticating the RFS of patients with SILADC after sublobectomy and can facilitate the selection of the optimal surgical treatment in these patients.

Acknowledgments

Funding: This study was supported by the Chongqing Medical Scientific Research Project (Joint Project of Chongqing Health Commission and Science and Technology Bureau; No. 2022MSXM147), the Chongqing Health Commission (Chongqing Talent Program-Innovation Leading Talent Research Project; No. CQYC20210303348), and the Chongqing Science and Technology Bureau (No. cstc2022ycjh-bgzxm0230).

Footnote

Reporting Checklist: The authors have completed the STROBE reporting checklist. Available at https://qims.amegroups.com/article/view/10.21037/qims-23-559/rc

Conflicts of Interest: All authors have completed the ICMJE uniform disclosure form (available at https://qims.amegroups.com/article/view/10.21037/qims-23-559/coif). The authors have no conflicts of interest to declare.

Ethical Statement: The authors are accountable for all aspects of the work in ensuring that questions related to the accuracy or integrity of any part of the work are appropriately investigated and resolved. The study was conducted in accordance with the Declaration of Helsinki (as revised in 2013). The retrospective cohort study was approved by the ethics committee of The First Affiliated Hospital of Chongqing Medical University, and the need for an informed consent was waived due to its retrospective nature.

References

1. Sung H, Ferlay J, Siegel RL, Laversanne M, Soerjomataram I, Jemal A, Bray F. Global Cancer Statistics 2020: GLOBOCAN Estimates of Incidence and Mortality Worldwide for 36 Cancers in 185 Countries. CA Cancer J Clin 2021;71:209-49.
2. de Koning HJ, van der Aalst CM, de Jong PA, Scholten ET, Nackaerts K, Heuvelmans MA, et al. Reduced Lung-Cancer Mortality with Volume CT Screening in a Randomized Trial. N Engl J Med 2020;382:503-13.
3. Jemal A, Fedewa SA. Lung Cancer Screening With Low-Dose Computed Tomography in the United States-2010 to 2015. JAMA Oncol 2017;3:1278-81.
4. Crinò L, Weder W, van Meerbeeck J, Felip E; ESMO Guidelines Working Group. Early stage and locally advanced (non-metastatic) non-small-cell lung cancer: ESMO Clinical Practice Guidelines for diagnosis, treatment and follow-up. Ann Oncol 2010;21 Suppl 5:v103-15.
5. Darling GE, Allen MS, Decker PA, Ballman K, Malthaner RA, Inculet RI, Jones DR, McKenna RJ, Landreneau RJ, Rusch VW, Putnam JB Jr. Randomized trial of mediastinal lymph node sampling versus complete lymphadenectomy during pulmonary resection in the patient with N0 or N1 (less than hilar) non-small cell carcinoma: results of the American College of Surgery Oncology Group Z0030 Trial. J Thorac Cardiovasc Surg 2011;141:662-70.
6. Altorki NK, Yip R, Hanaoka T, Bauer T, Aye R, Kohman L, Sheppard B, Thurer R, Andaz S, Smith M, Mayfield W, Grannis F, Korst R, Pass H, Straznicka M, Flores R, Henschke CI; I-ELCAP Investigators. Sublobar resection is equivalent to lobectomy for clinical stage 1A lung cancer in solid nodules. J Thorac Cardiovasc Surg 2014;147:754-62; Discussion 762-4.

7. Fiorelli A, Caronia FP, Daddi N, Loizzi D, Ampollini L, Ardò N, Ventura L, Carbognani P, Potenza R, Ardissone F, Sollitto F, Mattioli S, Puma F, Santini M, Ragusa M. Sublobar resection versus lobectomy for stage I non-small cell lung cancer: an appropriate choice in elderly patients? Surg Today 2016;46:1370-82.
8. Saji H, Okada M, Tsuboi M, Nakajima R, Suzuki K, Aokage K, et al. Segmentectomy versus lobectomy in small-sized peripheral non-small-cell lung cancer (JCOG0802/WJOG4607L): a multicentre, open-label, phase 3, randomised, controlled, non-inferiority trial. Lancet 2022;399:1607-17.
9. Altorki N, Wang X, Kozono D, Watt C, Landrenau R, Wigle D, et al. Lobar or Sublobar Resection for Peripheral Stage IA Non-Small-Cell Lung Cancer. N Engl J Med 2023;388:489-98.
10. Ettinger DS, Wood DE, Aisner DL, Akerley W, Bauman JR, Bharat A, et al. Non-Small Cell Lung Cancer, Version 3.2022, NCCN Clinical Practice Guidelines in Oncology. J Natl Compr Canc Netw 2022;20:497-530.
11. Nomori H, Horio H, Naruke T, Suemasu K. What is the advantage of a thoracoscopic lobectomy over a limited thoracotomy procedure for lung cancer surgery? Ann Thorac Surg 2001;72:879-84.
12. Asamura H, Hishida T, Suzuki K, Koike T, Nakamura K, Kusumoto M, Nagai K, Tada H, Mitsudomi T, Tsuboi M, Shibata T, Fukuda H; Japan Clinical Oncology Group Lung Cancer Surgical Study Group. Radiographically determined noninvasive adenocarcinoma of the lung: survival outcomes of Japan Clinical Oncology Group 0201. J Thorac Cardiovasc Surg 2013;146:24-30.
13. Liu Y, Kim J, Qu F, Liu S, Wang H, Balagurunathan Y, Ye Z, Gillies RJ. CT Features Associated with Epidermal Growth Factor Receptor Mutation Status in Patients with Lung Adenocarcinoma. Radiology 2016;280:271-80.
14. Mimae T, Miyata Y, Tsutani Y, Imai K, Ito H, Nakayama H, Ikeda N, Okada M. Wedge resection as an alternative treatment for octogenarian and older patients with early-stage non-small-cell lung cancer. Jpn J Clin Oncol 2020;50:1051-7.
15. Huang Y, Liu Z, He L, Chen X, Pan D, Ma Z, Liang C, Tian J, Liang C. Radiomics Signature: A Potential Biomarker for the Prediction of Disease-Free Survival in Early-Stage (I or II) Non-Small Cell Lung Cancer. Radiology 2016;281:947-57.
16. Kuhn E, Morbini P, Cancellieri A, Damiani S, Cavazza A, Comin CE. Adenocarcinoma classification: patterns and prognosis. Pathologica 2018;110:5-11.
17. Li Q, Li X, Li XY, He XQ, Chu ZG, Luo TY. Histological subtypes of solid-dominant invasive lung adenocarcinoma: differentiation using dual-energy spectral CT. Clin Radiol 2021;76:77.e1-7.
18. Niu R, Shao X, Shao X, Jiang Z, Wang J, Wang Y. Establishment and verification of a prediction model based on clinical characteristics and positron emission tomography/computed tomography (PET/CT) parameters for distinguishing malignant from benign ground-glass nodules. Quant Imaging Med Surg 2021;11:1710-22.
19. Xu L, Tavora F, Burke A. Histologic features associated with metastatic potential in invasive adenocarcinomas of the lung. Am J Surg Pathol 2013;37:1100-8.
20. Warth A, Muley T, Kossakowski CA, Goeppert B, Schirmacher P, Dienemann H, Weichert W. Prognostic Impact of Intra-alveolar Tumor Spread in Pulmonary Adenocarcinoma. Am J Surg Pathol 2015;39:793-801.
21. Moon Y, Sung SW, Moon SW, Park JK. Risk factors for recurrence after sublobar resection in patients with small (2 cm or less) non-small cell lung cancer presenting as a solid-predominant tumor on chest computed tomography. J Thorac Dis 2016;8:2018-26.
22. Dziedzic R, Zurek W, Marjanski T, Rudzinski P, Orlowski TM, Sawicka W, Marczyk M, Polanska J, Rzyman W. Stage I non-small-cell lung cancer: long-term results of lobectomy versus sublobar resection from the Polish National Lung Cancer Registry. Eur J Cardiothorac Surg 2017;52:363-9.
23. Hiramatsu M, Inagaki T, Inagaki T, Matsui Y, Satoh Y, Okumura S, Ishikawa Y, Miyaoka E, Nakagawa K. Pulmonary ground-glass opacity (GGO) lesions-large size and a history of lung cancer are risk factors for growth. J Thorac Oncol 2008;3:1245-50.
24. Lee HJ, Kim YT, Kang CH, Zhao B, Tan Y, Schwartz LH, Persigehl T, Jeon YK, Chung DH. Epidermal growth factor receptor mutation in lung adenocarcinomas: relationship with CT characteristics and histologic subtypes. Radiology 2013;268:254-64.
25. Sun F, Huang Y, Yang X, Zhan C, Xi J, Lin Z, Shi Y, Jiang W, Wang Q. Solid component ratio influences prognosis of GGO-featured IA stage invasive lung adenocarcinoma. Cancer Imaging 2020;20:87.
26. Zhang BW, Zhang Y, Ye JD, Qiang JW. Use of relative CT values to evaluate the invasiveness of pulmonary subsolid nodules in patients with emphysema. Quant Imaging Med Surg 2021;11:204-14.
27. Sawabata N, Kanzaki R, Sakamoto T, Kusumoto H, Kimura T, Nojiri T, Kawamura T, Susaki Y, Funaki S,

Nakagiri T, Shintani Y, Inoue M, Minami M, Okumura M. Clinical predictor of pre- or minimally invasive pulmonary adenocarcinoma: possibility of sub-classification of clinical T1a. Eur J Cardiothorac Surg 2014;45:256-61.
28. Lee MA, Kang J, Lee HY, Kim W, Shon I, Hwang NY, Kim HK, Choi YS, Kim J, Zo JI, Shim YM. Spread through air spaces (STAS) in invasive mucinous adenocarcinoma of the lung: Incidence, prognostic impact, and prediction based on clinicoradiologic factors. Thorac Cancer 2020;11:3145-54.
29. Aly RG, Rekhtman N, Li X, Takahashi Y, Eguchi T, Tan KS, Rudin CM, Adusumilli PS, Travis WD. Spread Through Air Spaces (STAS) Is Prognostic in Atypical Carcinoid, Large Cell Neuroendocrine Carcinoma, and Small Cell Carcinoma of the Lung. J Thorac Oncol 2019;14:1583-93.
30. Yokoyama S, Murakami T, Tao H, Onoda H, Hara A, Miyazaki R, Furukawa M, Hayashi M, Inokawa H, Okabe K, Akagi Y. Tumor Spread Through Air Spaces Identifies a Distinct Subgroup With Poor Prognosis in Surgically Resected Lung Pleomorphic Carcinoma. Chest 2018;154:838-47.
31. Ma J, Yang YL, Wang Y, Zhang XW, Gu XS, Wang ZC. Relationship between computed tomography morphology and prognosis of patients with stage I non-small cell lung cancer. Onco Targets Ther 2017;10:2249-56.
32. Choe J, Kim MY, Yun JK, Lee GD, Kim YH, Choi S, Kim DK. Sublobar Resection in Stage IA Non-Small Cell Lung Cancer: Role of Preoperative CT Features in Predicting Pathologic Lymphovascular Invasion and Postoperative Recurrence. AJR Am J Roentgenol 2021;217:871-81.
33. Huo JW, Huang XT, Li X, Gong JW, Luo TY, Li Q. Pneumonic-type lung adenocarcinoma with different ranges exhibiting different clinical, imaging, and pathological characteristics. Insights Imaging 2021;12:169.
34. Okada S, Hattori A, Matsunaga T, Takamochi K, Oh S, Inoue M, Suzuki K. Prognostic value of visceral pleural invasion in pure-solid and part-solid lung cancer patients. Gen Thorac Cardiovasc Surg 2021;69:303-10.
35. Ahn SY, Park CM, Jeon YK, Kim H, Lee JH, Hwang EJ, Goo JM. Predictive CT Features of Visceral Pleural Invasion by T1-Sized Peripheral Pulmonary Adenocarcinomas Manifesting as Subsolid Nodules. AJR Am J Roentgenol 2017;209:561-6.
36. Hsu JS, Han IT, Tsai TH, Lin SF, Jaw TS, Liu GC, Chou SH, Chong IW, Chen CY. Pleural Tags on CT Scans to Predict Visceral Pleural Invasion of Non-Small Cell Lung Cancer That Does Not Abut the Pleura. Radiology 2016;279:590-6.

Cite this article as: Huo J, Luo T, Lv F, Li Q. Clinicopathological and computed tomography features associated with recurrence-free survival of patients with small-sized peripheral invasive lung adenocarcinoma after sublobectomy. Quant Imaging Med Surg 2023;13(12):8144-8156. doi: 10.21037/qims-23-559

